



## Novel Triazolo[4,3-*a*]pyrazines as Potential MmpL3 Inhibitors: Design, Synthesis, Antitubercular Evaluation and Molecular Docking Studies

JAYASHREE KSHIRSAGAR<sup>1,2</sup>, WILSON CHANDANE<sup>3</sup>, DIPAK HIWARALE<sup>4</sup>, NITIN NAIK<sup>5</sup>,  
KAILAS SONAWANE<sup>5</sup>, GAJANAN RASHINKAR<sup>3</sup>, RAJASHRI SALUNKHE<sup>3</sup> and SUNITA SHIRKE<sup>1,\*</sup>

<sup>1</sup>Department of Chemistry, Vivekanand College, Kolhapur-416003, India

<sup>2</sup>Department of Chemistry, The New College, Kolhapur-416012, India

<sup>3</sup>Department of Chemistry, Shivaji University, Kolhapur-416004, India

<sup>4</sup>Department of Chemistry, Vishwasrao Naik Arts, Commerce and Baba Naik Science Mahavidyalaya, Shirala-415408, India

<sup>5</sup>Department of Microbiology, Shivaji University, Kolhapur-416004, India

\*Corresponding author: Tel: +91 231 265 8612; E-mail: [sds.orgchem@gmail.com](mailto:sds.orgchem@gmail.com)

Received: 5 September 2024;

Accepted: 24 October 2024;

Published online: 30 November 2024;

AJC-21822

A series of biologically active novel triazolo[4,3-*a*]pyrazines (**5a-f**) were synthesized and characterized by spectroscopic techniques. The synthesized compounds **5a-f** were evaluated for their *in vitro* anti-tubercular (anti-TB) activity against drug-sensitive Mtb H37Rv (ATCC 27294) strain as well as two drug-resistant Mtb strains *viz.* Mtb H37Rv ATCC 35822 (INH-resistant) and Mtb H37Rv ATCC 35837 (ETH-resistant). The synthesized compounds **5a-f** displayed good to moderate anti-TB activity against drug-sensitive, INH-resistant and ETH-resistant Mtb H37Rv strains. Among all the compounds tested, compound **5c** was found to be significantly potent. It inhibited the growth of drug-sensitive, INH-resistant and ETH-resistant Mtb H37Rv strains with MIC values  $0.59 \pm 0.11 \mu\text{M}$ ,  $20.83 \pm 0.67 \mu\text{M}$  and  $15.37 \pm 0.14 \mu\text{M}$ , respectively. Moreover, compounds **5a-f** were also tested for their cytotoxic efficacy against the mammalian Vero cell line at a maximum concentration of 50  $\mu\text{M}$ . Molecular docking experiments of compounds **5a-f** with the mycobacterial membrane protein large 3 (MmpL3) were performed to justify the biological activity and provide insight into the possible mechanism of action and binding mode of compounds. *In silico* predictions were used to validate compound toxicity descriptors, drug scores and drug-likeness properties.

**Keywords:** Pyrazine, Tuberculosis, Cytotoxicity, Molecular docking, Drug-likeness.

### INTRODUCTION

Tuberculosis (TB) is a widely spread and highly communicable respiratory disease, that has significant implications for human health [1,2]. It stands as one of the primary causes of global mortality, second only to HIV/AIDS [3]. *Mycobacterium tuberculosis* (Mtb) is the causative agent of TB, a bacterium that primarily affects the respiratory system but can remain asymptomatic for extended periods [4]. The WHO estimates that approximately one-fourth of the world's population has been infected with Mtb, resulting in around 8 million cases of active TB and nearly 2 million deaths each year [5]. The standard treatment for TB entails a six-month regimen of first-line anti-tubercular drugs including isoniazid, rifampin, ethambutol and pyrazinamide (PZA). However, it has been shown that patients do not adhere to the recommended longer treatment period [6],

contributing to the emergence of drug-resistant strains of Mtb, including multidrug-resistant (MDR) and extensively drug-resistant (XDR) Mtb [7]. Consequently, the development of novel compounds to combat drug-resistant Mtb strains is a pressing challenge in the field of drug research. Furthermore, current TB therapies exhibit diminished efficacy, heightened toxicity and adverse side effects, leading to increased mortality rates, particularly among individuals infected with HIV [8]. This has spurred efforts to identify new therapeutic targets and create alternative anti-TB medications.

In recent years, computational chemistry has become a focal point for chemists worldwide [9]. This discipline employs computer programs based on principles of theoretical chemistry to examine intricate chemical structures [10]. Computational techniques such as machine learning [11], molecular fingerprints [12], density functional theory (DFT), molecular docking,

molecular dynamics simulations and *in silico* ADMET analysis [13] are used to scrutinize molecular structures, interactions and properties. Molecular docking, in particular, has been extensively employed in computer-assisted drug discovery, aiding in the prediction of ligand binding modes and affinities with known protein structures [14,15]. As a result, it streamlines research efforts and reduces costs [16,17].

Heterocyclic compounds, due to their diverse biological activities, are vital in the discovery of new drugs [18]. Nitrogen containing heterocycles, in particular, have garnered considerable attention in the field of medicinal chemistry due to their therapeutic potential [19]. Among these, the pyrazine nucleus has emerged as a fundamental framework in the development of novel drug molecules [20,21]. Pyrazine derivatives, especially triazolo[4,3-*a*]pyrazines, have attracted interest due to their diverse biological and pharmacological activities [22].

The versatile structure, facile synthesis, ease of functionalization and therapeutic potential of triazolo[4,3-*a*]pyrazines present opportunities for the development of libraries of biologically active compounds. Building upon ongoing research into the development of novel heterocycles [23,24], we report, herein the synthesis of novel triazolo[4,3-*a*]pyrazines (**5a-f**) (Scheme-I). These compounds were assessed for their *in vitro* antitubercular activity against *Mycobacterium tuberculosis* (Mtb) H37Rv strains, along with evaluations of physico-chemical properties, cytotoxicity and pharmacokinetics. Additionally, the molecular docking simulations were conducted to elucidate the interactions between potent compounds and the binding pocket of mycobacterial membrane protein large 3 (MmpL3).

## EXPERIMENTAL

All chemicals and reagents were procured from commercial suppliers and used without further purification. Fourier Transform Infrared (FTIR) spectra were measured on Perkin-Elmer One FTIR spectrophotometer using KBr discs ( $\approx 5\%$  w/w).  $^1\text{H}$  NMR spectra were recorded with a Bruker Avance (400 MHz for  $^1\text{H}$  NMR) spectrometer using DMSO- $d_6$  as solvent and tetramethylsilane as an internal standard. Mass spectra were recorded with a PE Sciex API300 mass spectrophotometer. Elemental analysis was performed using a Perkin-Elmer type 240 C analyzer. Melting points were determined on a Shimadzu DSC-50 instrument and are uncorrected.

**Synthesis of 3-methyl[1,2,4]triazolo[4,3-*a*]pyrazine (2):** Initially, 3-methyl[1,2,4]triazolo[4,3-*a*]pyrazine (**2**) was synthesized by adopting the literature procedure with slight modification [25]. Accordingly, acetaldehyde (5 mmol) was added to a solution of 2-hydrazineylpyrazine (**1**) (5 mmol) in ethanol (30 mL) while stirring. The reaction mixture was stirred at room temperature for 1 h. After the completion of the reaction, as indicated by thin-layer chromatography (TLC), chloramine-T trihydrate (5 mmol) was added to the reaction mixture. The resultant reaction mixture was refluxed at 60 °C until the formation of product as indicated by TLC [26]. Finally, the reaction mixture was diluted with ice-cold water to obtain a solid precipitate which was filtered, washed several times with distilled water as well as ethanol and dried in air to obtain pure 3-methyl-

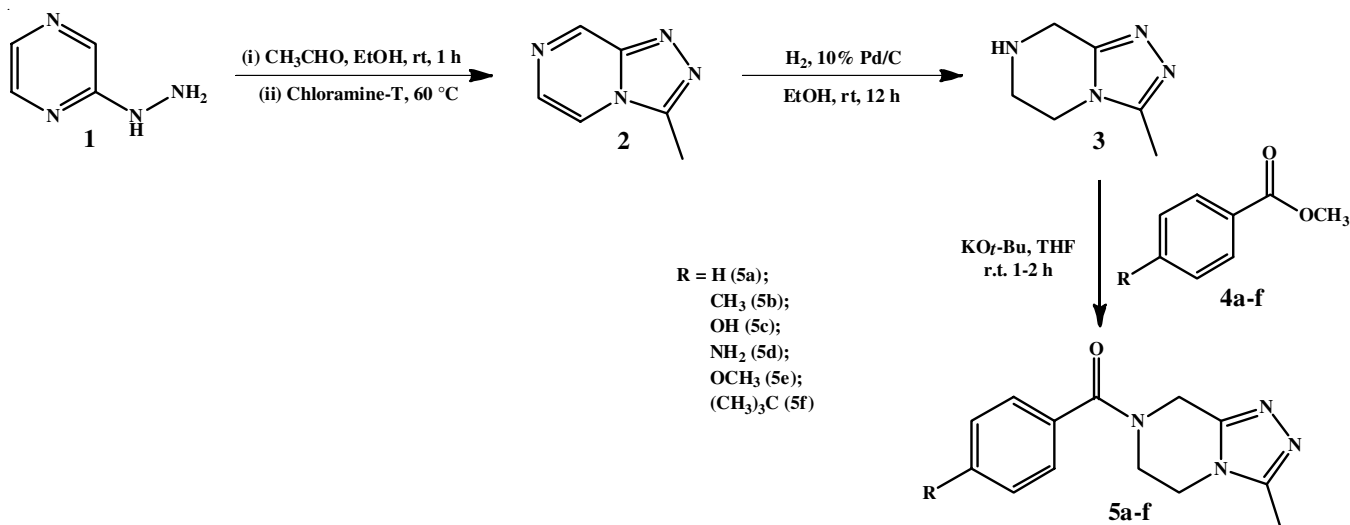
[1,2,4]triazolo[4,3-*a*]pyrazine (**2**). Yield: 75%; elemental analysis for  $\text{C}_6\text{H}_6\text{N}_4$ , calcd. (found) %: C, 53.72 (53.71); H, 4.51 (4.48); N, 41.77 (41.79)  $^1\text{H}$  NMR (400 MHz, DMSO- $d_6$ )  $\delta$  ppm: 2.32 (s, 3H, -CH<sub>3</sub>), 8.61 (d,  $J = 7.1$  Hz, 1H, Ar-H), 8.67 (d,  $J = 6.7$  Hz, 1H, Ar-H), 8.72 (s, 1H, Ar-H); MS:  $m/z$  135.1 (M+1).

**Synthesis of 3-methyl-5,6,7,8-tetrahydro-[1,2,4]triazolo[4,3-*a*]pyrazine (3):** The synthesis of 3-methyl-5,6,7,8-tetrahydro[1,2,4]triazolo[4,3-*a*]pyrazine (**3**) was carried out as per the procedure reported in the literature [27]. Accordingly, a solution of compound **2** (2 mmol) in ethanol (20 mL) was hydrogenated using atmospheric hydrogen in the presence of 0.5 g 10% Pd/C catalyst at room temperature for 12 h. The reaction mixture was filtered over a celite bed to remove the traces of water and evaporation of solvent in a vacuum, followed by column chromatography (MeOH:DCM, 20:80 v/v) afforded pure 3-methyl-5,6,7,8-tetrahydro[1,2,4]triazolo[4,3-*a*]pyrazine (**3**). Yield: 79%; elemental analysis for  $\text{C}_6\text{H}_{10}\text{N}_4$ , calcd. (found) %: C, 52.16 (52.13); H, 7.30 (7.27); N, 40.55 (40.59);  $^1\text{H}$  NMR (400 MHz, DMSO- $d_6$ )  $\delta$  ppm: 1.93 (s, 1H, -NH), 2.32 (s, 3H, -CH<sub>3</sub>), 3.08 (t,  $J = 6.2$  Hz, 2H, -CH<sub>2</sub>), 3.91 (s, 2H, -CH<sub>2</sub>), 4.12 (t,  $J = 10.2$  Hz, 2H, -CH<sub>2</sub>); MS:  $m/z$  139 (M+1).

**Synthesis of triazolo[4,3-*a*]pyrazines (5a-f):** The triazolo[4,3-*a*]pyrazines (**5a-f**) were synthesized by following the procedure described elsewhere [28]. Accordingly, potassium *tert*-butoxide (KO $t$ -Bu) (2.0 mmol) was dissolved in THF (15 mL) with constant stirring. The substituted methyl benzoate (1 mmol) and compound **3** (1 mmol) were mixed immediately and the reaction mixture was stirred at room temperature until the completion of reaction as indicated by TLC. After evaporation of THF in vacuum; distilled water (15 mL) and dichloromethane (15 mL) were added and the organic layer was separated and dried over anhydrous Na<sub>2</sub>SO<sub>4</sub>. Finally, the evaporation of solvent in vacuum followed by column chromatography over silica gel using ethyl acetate:*n*-hexane (1:3) mixture afforded pure products (Scheme-I).

**(3-Methyl-5,6-dihydro[1,2,4]triazolo[4,3-*a*]pyrazin-7(8H)-yl(phenyl)methanone (5a):** Yield: 89%; m.p.: 151-153 °C; elemental analysis for  $\text{C}_{13}\text{H}_{14}\text{N}_4\text{O}$ , calcd. (found) %: C, 64.45 (64.42); H, 5.82 (5.78); N, 23.13 (23.17); IR (KBr,  $\nu_{\text{max}}$ , cm<sup>-1</sup>): 1786, 1528, 1495;  $^{13}\text{C}$  NMR (100 MHz, DMSO- $d_6$ )  $\delta$  ppm: 11.4, 33.2, 48.5, 50.5, 127.2, 128.5, 129.7, 135.2, 149.6, 163.8, 171.1;  $^1\text{H}$  NMR (400 MHz, DMSO- $d_6$ )  $\delta$  ppm: 2.32 (s, 3H, -CH<sub>3</sub>), 3.53 (t,  $J = 6.7$  Hz, 2H, -CH<sub>2</sub>), 4.28 (t,  $J = 9.8$  Hz, 2H, -CH<sub>2</sub>), 4.81 (s, 2H, -CH<sub>2</sub>), 7.54 (t,  $J = 8.2$  Hz, 2H, Ar-H), 7.62 (t,  $J = 7.6$  Hz, 1H, Ar-H), 7.95 (d,  $J = 6.7$  Hz, 2H, Ar-H); MS:  $m/z$  243 (M+1).

**(3-Methyl-5,6-dihydro[1,2,4]triazolo[4,3-*a*]pyrazin-7(8H)-yl(*p*-tolyl)methanone (5b):** Yield: 91%; m.p.: 162-164 °C; elemental analysis for  $\text{C}_{14}\text{H}_{16}\text{N}_4\text{O}$ , calcd. (found) %: C, 65.61 (65.58); H, 6.29 (6.26); N, 21.86 (21.89); IR (KBr,  $\nu_{\text{max}}$ , cm<sup>-1</sup>): 1781, 1518, 1493;  $^1\text{H}$  NMR (400 MHz, DMSO- $d_6$ )  $\delta$  ppm: 2.32 (s, 3H, -CH<sub>3</sub>), 2.41 (s, 3H, -CH<sub>3</sub>), 3.53 (t,  $J = 6.5$  Hz, 2H, -CH<sub>2</sub>), 4.29 (t,  $J = 10.2$  Hz, 2H, -CH<sub>2</sub>), 4.79 (s, 2H, -CH<sub>2</sub>), 7.22 (d,  $J = 4.2$  Hz, 2H, Ar-H), 7.64 (d,  $J = 4.7$  Hz, 2H, Ar-H);  $^{13}\text{C}$  NMR (100 MHz, DMSO- $d_6$ )  $\delta$  ppm: 11.4, 21.3, 33.2, 48.5, 50.5, 127.1, 128.8, 132.2, 139.4, 149.6, 163.7, 171.1; MS:  $m/z$  257 (M+1).



Scheme-I: Synthesis of novel triazolo[4,3-*a*]pyrazines (5a-f)

**(4-Hydroxyphenyl)(3-methyl-5,6-dihydro[1,2,4]-triazolo[4,3-*a*]pyrazin-7(8*H*)-yl)methanone (5c):** Yield: 87%; m.p.: 148-150 °C; elemental analysis for  $\text{C}_{13}\text{H}_{14}\text{N}_4\text{O}_2$ , calcd. (found) %: C, 60.45 (60.41); H, 5.46 (5.43); N, 21.69 (21.74); IR (KBr,  $\nu_{\text{max}}$ ,  $\text{cm}^{-1}$ ): 3508, 1786, 1508, 1481;  $^1\text{H}$  NMR (400 MHz, DMSO- $d_6$ )  $\delta$  ppm: 2.32 (s, 3H, -CH<sub>3</sub>), 3.50 (t,  $J$  = 6.8 Hz, 2H, -CH<sub>2</sub>), 4.30 (t,  $J$  = 8.6 Hz, 2H, -CH<sub>2</sub>), 4.84 (s, 2H, -CH<sub>2</sub>), 5.58 (s, 1H, -OH), 7.16 (d,  $J$  = 2.6 Hz, 2H, Ar-H), 7.80 (d,  $J$  = 3.2 Hz, 2H, Ar-H);  $^{13}\text{C}$  NMR (100 MHz, DMSO- $d_6$ )  $\delta$  ppm: 11.4, 33.2, 48.5, 50.5, 115.7, 127.8, 128.6, 149.6, 159.5, 163.8, 171.1; MS:  $m/z$  259 (M+1).

**(4-Aminophenyl)(3-methyl-5,6-dihydro[1,2,4]triazolo[4,3-*a*]pyrazin-7(8*H*)-yl)methanone (5d):** Yield: 85%; m.p.: 145-147 °C; elemental analysis for  $\text{C}_{13}\text{H}_{15}\text{N}_5\text{O}$ , calcd. (found) %: C, 60.69 (60.67); H, 5.88 (5.84); N, 27.22 (27.25); IR (KBr,  $\nu_{\text{max}}$ ,  $\text{cm}^{-1}$ ): 3248, 1716, 1512, 1492;  $^1\text{H}$  NMR (400 MHz, DMSO- $d_6$ )  $\delta$  ppm: 2.36 (s, 3H, -CH<sub>3</sub>), 3.40 (t,  $J$  = 2.7 Hz, 2H, -CH<sub>2</sub>), 4.31 (t,  $J$  = 10.5 Hz, 2H, -CH<sub>2</sub>), 4.86 (s, 2H, -CH<sub>2</sub>), 5.96 (s, 2H, -NH<sub>2</sub>), 7.38 (d,  $J$  = 2.1 Hz, 2H, Ar-H), 7.75 (d,  $J$  = 4.0 Hz, 2H, Ar-H);  $^{13}\text{C}$  NMR (100 MHz, DMSO- $d_6$ )  $\delta$  ppm: 11.4, 33.2, 48.5, 50.5, 114.1, 125.2, 129.8, 149.4, 149.7, 163.7, 171.1; MS:  $m/z$  258 (M+1).

**(4-Methoxyphenyl)(3-methyl-5,6-dihydro-[1,2,4]-triazolo[4,3-*a*]pyrazin-7(8*H*)-yl)methanone (5e):** Yield: 90%; m.p.: 156-158 °C; elemental analysis for  $\text{C}_{14}\text{H}_{16}\text{N}_4\text{O}_2$ , calcd. (found) %: C, 61.75 (61.72); H, 5.92 (5.02); N, 20.58 (20.63); IR (KBr,  $\nu_{\text{max}}$ ,  $\text{cm}^{-1}$ ): 1762, 1528, 1487;  $^1\text{H}$  NMR (400 MHz, DMSO- $d_6$ )  $\delta$  ppm: 2.33 (s, 3H, -CH<sub>3</sub>), 3.52 (t,  $J$  = 7.2 Hz, 2H, -CH<sub>2</sub>), 3.81 (s, 3H, -OCH<sub>3</sub>), 4.31 (t,  $J$  = 10.1 Hz, 2H, -CH<sub>2</sub>), 4.83 (s, 2H, -CH<sub>2</sub>), 7.28 (d,  $J$  = 6.4 Hz, 2H, Ar-H), 7.72 (d,  $J$  = 4.9 Hz, 2H, Ar-H);  $^{13}\text{C}$  NMR (100 MHz, DMSO- $d_6$ )  $\delta$  ppm: 11.4, 33.2, 48.5, 50.5, 55.4, 114.1, 127.5, 128.2, 149.7, 161.6, 163.7, 171.1; MS:  $m/z$  273 (M+1).

**4-(*tert*-Butyl)phenyl)(3-methyl-5,6-dihydro[1,2,4]-triazolo[4,3-*a*]pyrazin-7(8*H*)-yl)methanone (5f):** Yield: 84%; m.p.: 166-168 °C; elemental analysis for  $\text{C}_{17}\text{H}_{22}\text{N}_4\text{O}$ , calcd. (found) %: C, 68.43 (68.41); H, 7.43 (7.39); N, 18.78 (18.82); IR (KBr,  $\nu_{\text{max}}$ ,  $\text{cm}^{-1}$ ): 1706, 1521, 1487;  $^1\text{H}$  NMR (400

MHz, DMSO- $d_6$ )  $\delta$  ppm: 1.33 (s, 9H, -(CH<sub>3</sub>)<sub>3</sub>), 2.32 (s, 3H, -CH<sub>3</sub>), 3.65 (t,  $J$  = 6.8 Hz, 2H, -CH<sub>2</sub>), 4.28 (t,  $J$  = 10.0 Hz, 2H, -CH<sub>2</sub>), 4.87 (s, 2H, -CH<sub>2</sub>), 7.21 (d,  $J$  = 8.4 Hz, 2H, Ar-H), 7.82 (d,  $J$  = 8.0 Hz, 2H, Ar-H);  $^{13}\text{C}$  NMR (100 MHz, DMSO- $d_6$ )  $\delta$  ppm: 11.4, 31.3, 33.2, 34.2, 48.5, 50.5, 124.8, 126.8, 132.1, 149.6, 152.3, 163.7, 171.1; MS:  $m/z$  299 (M+1).

**Antitubercular activity:** Novel triazolo[4,3-*a*]pyrazines were tested for their *in vitro* anti-tubercular (anti-TB) activity against drug-sensitive Mtb H37Rv (ATCC 27294) strain as well as two significant drug-resistant Mtb strains *viz.* Mtb H37Rv ATCC 35822 (INH-resistant) and Mtb H37Rv ATCC 35837 (ETH-resistant). An agar dilution technique was employed to determine the minimum inhibitory concentration (MIC) [29]. The bacterial growth rate was assessed visually after the incubation period of 28 days at 37 °C.

**Cytotoxicity assay:** Cytotoxicity assay of novel triazolo[4,3-*a*]pyrazines (5a-f) against mammalian Vero cell line was carried out using an MTT-based *in vitro* toxicology assay kit [30]. At a density of  $1 \times 10^5$  cells per well, cells were seeded. After 24 h, cells were treated for 48 h with varied concentrations (0-50  $\mu\text{M}$ ) of test compounds. A 20  $\mu\text{L}$  of MTT (5 mg/mL) was added to each well and incubated for 4 h at 37 °C. After carefully removing the medium, 40  $\mu\text{L}$  of DMSO was added to each well. The plates were examined using an ELISA plate reader at a wavelength of 595 nm. The IC<sub>50</sub> values of substances in the cell lines were computed using the Prism 7 programme. The experiments were carried out in triplicate.

**Molecular docking:** The three dimensional crystal structure of mycobacterial membrane protein large 3 (MmpL3) (PDB ID: 6AJJ) was downloaded from the RCSB protein data bank website <https://www.rcsb> [31,32] and used as a receptor to perform molecular docking with synthesized compounds 5a-f. The molecular docking of the synthesized compounds 5a-f with the receptor protein 6AJJ was performed using AutoDock-4.2 [33-38]. Moreover, CASTp is an online tool that determines empty cavities on the surface of proteins. The active site within the receptor was identified using CASTp [39]. The grid dimensions were set to 80 Å × 80 Å × 80 Å, which accommodates

the active site. Grid centre was selected at X = 1.365, Y = 11.715, Z = 37.367 coordinates with 0.02 rate of mutation and 0.8 crossing over rate. The grid spacing of 0.375 Å was centred on the binding site pocket, which covers all the active site residues of the receptor molecule. The step size of 2.0 Å for translation and 10° for rotation was selected. The maximum number of energy evaluations was set to 2500000. The population size was fixed to 150 to generate 100 conformations for 27000 generations using Lamarckian Genetic Algorithm.

The best-docked conformation among 100 conformations was obtained with the least binding energy values. Ligand-receptor interactions were visualized with AutoDock and UCSF Chimera [40]. In addition, 2D interaction images were generated using LigPlot [41,42].

**Drug-likeness prediction:** Lipinski's rule of five [43] was used to predict the drug-likeness properties of the novel triazolo[4,3-*a*]pyrazines (**5a-f**) using a free online resource <http://www.swissadme.ch>.

## RESULTS AND DISCUSSION

Initially, a hydrazone of 2-hydrazineylpyrazine (**1**) was generated *in situ* by condensation of 2-hydrazineylpyrazine (**1**) with acetaldehyde in ethanol at room temperature. The hydrazone thus formed on treatment with chloramine-T trihydrate at 60 °C afforded the desired 3-methyl-[1,2,4]triazolo[4,3-*a*]pyrazine (**2**) *via* oxidative cyclization. In second step, compound **2** was hydrogenated in the presence of ambient hydrogen at room temperature in the presence of 10% Pd/C to give 3-methyl-5,6,7,8-tetrahydro-[1,2,4]triazolo[4,3-*a*]pyrazine (**3**). Finally, The synthesis of triazolo[4,3-*a*]pyrazines (**5a-f**) was carried out *via* KOt-Bu assisted amidation of substituted methyl benzoates (**4a-f**) with compound **3** in THF at room temperature. For the optimization of reaction conditions, the reaction between compound **3** and methyl benzoate (**4a**) was chosen as model reaction. Initially, the optimization of base catalyst for model reaction was performed using various base catalysts (Table-1). It was observed that when the model reaction was carried out in the absence of base catalyst, only trace amount of the desired product was formed even after 24 h of reaction time (Table-1, entry 1). But in the presence of base catalyst (2 equiv.) the model reaction afforded good to better yields. The bases such as Na<sub>2</sub>CO<sub>3</sub> and K<sub>2</sub>CO<sub>3</sub> gave poor yields (Table-1, entries

TABLE-1  
OPTIMIZATION DATA OF BASE CATALYST IN THE  
SYNTHESIS OF TRIAZOLO[4,3-*a*]PYRAZINES<sup>a</sup>

Entry	Base (equiv.)	Time (min)	Yield <sup>b</sup> (%)
1	–	1440	Trace
2	Na <sub>2</sub> CO <sub>3</sub> (2)	180	49
3	K <sub>2</sub> CO <sub>3</sub> (2)	180	56
4	NaOH (2)	120	63
5	KOH (2)	120	67
6	NaOt-Bu (2)	80	76
7	KOt-Bu (2)	60	89
8	KOt-Bu (1)	90	68

<sup>a</sup>Reaction conditions: Compound **3** (1.0 mmol), methyl benzoate **4a** (1.0 mmol), base catalyst (1/2 equiv.), THF (5.0 mL), room temperature. <sup>b</sup>Isolated yield.

2-3), while NaOH, KOH and KOt-Bu (1 equiv.) afforded moderate yields of the desired product (Table-1, entries 4,5 and 8). NaOt-Bu gave good yield of the desired product (Table-1, entry 6). A significant increase up to 89% in the yield of the desired product was achieved with KOt-Bu (2 equiv.) (Table-1, entry 7). Therefore, KOt-Bu (2 equiv.) was chosen as a catalyst for further optimization studies.

Next, the solvent optimization was carried out by testing various solvents for the model reaction (Table-2). Poor yields of the desired product were obtained in *n*-hexane, cyclohexane and toluene (Table-2, entries 4-6). DMF afforded moderate yield (Table-2, entry 1), while diethyl ether gave good yield. A noteworthy increase in the yield (89%) of the desired product was observed for THF (Table-2, entry 2), therefore, it was chosen as a solvent for synthesis of triazolo[4,3-*a*]pyrazines.

TABLE-2  
OPTIMIZATION DATA OF SOLVENT IN THE  
SYNTHESIS OF TRIAZOLO[4,3-*a*]PYRAZINES<sup>a</sup>

Entry	Solvent	Time (min)	Yield <sup>b</sup> (%)
1	DMF	80	61
2	THF	60	89
3	Et <sub>2</sub> O	60	74
4	<i>n</i> -Hexane	90	48
5	Cyclohexane	120	36
6	Toluene	120	42

<sup>a</sup>Reaction conditions: Compound **3** (1.0 mmol), methyl benzoate **4a** (1.0 mmol), KOt-Bu catalyst (2 equiv.), solvent (5.0 mL), room temperature. <sup>b</sup>Isolated yield.

After optimization of reaction conditions, the general scope of the protocol was tested by reacting compound **3** with substituted methyl benzoates (**4a-f**) having electron donating groups. 4-Methyl and 4-methoxy substituted methyl benzoates afforded excellent yields (91% and 90%, respectively) of the desired product (Table-3, entries b-e). A slight decrease in the yield (87% and 85%) was observed for 4-hydroxy and 4-amino substituted methyl benzoates, respectively (Table-3, entries c-d), while 4-(*t*-butyl)methyl benzoate afforded the lowest yield (84%) of desired product (Table-3, entry f).

TABLE-3  
SYNTHESIS OF NOVEL TRIAZOLO[4,3-*a*]PYRAZINES (**5a-f**)<sup>a</sup>

Entry	Substituted methyl benzoate ( <b>4</b> )	Product ( <b>5</b> )	Time (min)	Yield <sup>b</sup> (%)
a	H	<b>5a</b>	60	89
b	CH <sub>3</sub>	<b>5b</b>	80	91
c	OH	<b>5c</b>	90	87
d	NH <sub>2</sub>	<b>5d</b>	80	85
e	OCH <sub>3</sub>	<b>5e</b>	80	90
f	(CH <sub>3</sub> ) <sub>3</sub> C	<b>5f</b>	90	84

<sup>a</sup>Reaction conditions: Compound **3** (1.0 mmol), substituted methyl benzoate **4a-f** (1.0 mmol), KOt-Bu (2 equiv.), THF (5.0 mL), room temperature; <sup>b</sup>Isolated yields

The structures of compounds **2**, **3** and novel triazolo[4,3-*a*]pyrazines (**5a-f**) were confirmed on the basis of FT-IR, <sup>1</sup>H NMR and mass spectrometry. The spectral data are in good agreement with the proposed structures. The <sup>1</sup>H NMR spectrum of compound **2** displayed a singlet at δ 2.32 ppm for methyl protons,

while the mass spectrum gave  $m/z = 135.1$  for (M+1) peak confirming the formation of compound **2**. Similarly,  $^1\text{H NMR}$  spectrum of compound **3** displayed a singlet at  $\delta$  3.91 ppm for methylene protons, two triplets at  $\delta$  3.08 and 4.12 ppm for two  $-\text{CH}_2$  groups adjacent to each other and a singlet at  $\delta$  1.93 ppm for the  $-\text{NH}$  proton. The FT-IR spectra of novel triazolo[4,3-*a*]pyrazines (**5a-f**) displayed characteristic bands between 1786 to 1702  $\text{cm}^{-1}$ , suggesting the presence of a carbonyl group. Furthermore, the IR spectra of compounds **5c** and **5d** revealed absorption bands at 3508 and 3248  $\text{cm}^{-1}$  attributed to the stretching vibrations of  $-\text{OH}$  and  $-\text{NH}_2$  groups, respectively. The absence of signal for  $-\text{NH}$  proton in the  $^1\text{H NMR}$  spectra of novel triazolo[4,3-*a*]pyrazines (**5a-f**) confirmed the successful condensation of compound **3** with substituted methyl benzoates (**4a-f**). Additionally, signals for aromatic protons were observed between  $\delta$  7.16 to 7.95 ppm. Moreover, the [M+1] peaks in the mass spectra of novel triazolo[4,3-*a*]pyrazines (**5a-f**) were matched with their fragmentation pattern.

**Antitubercular activity:** Initially, novel triazolo[4,3-*a*]pyrazines (**5a-f**) were evaluated for their *in vitro* anti-tubercular (anti-TB) activity against drug-sensitive Mtb H37Rv (ATCC 27294) strain using an agar dilution technique. The results are summarized in Table-4. The MIC values of the standard drugs, *viz.* isoniazid (INH) and ethambutol (ETH), were also determined. The novel triazolo[4,3-*a*]pyrazines (**5a-f**) displayed moderate to good anti-TB activity compared to the standard drugs INH and ETH. The MIC values of the synthesized compounds (**5a-f**) were found to be in the range of 0.59 to 6.12  $\mu\text{M}$ . When compared to ETH (MIC =  $5.01 \pm 0.17 \mu\text{M}$ ); compounds **5c** (MIC =  $0.59 \pm 0.11 \mu\text{M}$ ) and **5d** (MIC =  $0.97 \pm 0.16 \mu\text{M}$ ) demonstrated potent, compound **5e** (MIC =  $1.28 \pm 0.59 \mu\text{M}$ ) displayed good, compounds **5f** (MIC =  $2.05 \pm 1.02 \mu\text{M}$ ) and **5b** (MIC =  $3.14 \pm 0.69 \mu\text{M}$ ) exhibited moderate, while compound **5a** (MIC =  $6.12 \pm 1.08 \mu\text{M}$ ) displayed poor anti-TB activity against drug-sensitive Mtb H37Rv (ATCC 27294) strain. Furthermore, it was observed that the synthesized compounds **5a-f** exhibited lower efficacy in inhibiting the growth of drug sensitive Mtb H37Rv (ATCC 27294) strain as compared to INH (MIC =  $0.36 \pm 0.09 \mu\text{M}$ ).

TABLE-4  
ANTI-TUBERCULAR ACTIVITY DATA OF **5a-f** AGAINST  
DRUG-SENSITIVE Mtb H37Rv (ATCC 27294) STRAIN

Compound	Mtb H37Rv <sup>a</sup> MIC ( $\mu\text{M}$ ) <sup>b</sup>	ClogP
<b>5a</b>	$6.12 \pm 1.08$	1.30
<b>5b</b>	$3.14 \pm 0.69$	1.65
<b>5c</b>	$0.59 \pm 0.11$	0.96
<b>5d</b>	$0.97 \pm 0.16$	0.63
<b>5e</b>	$1.28 \pm 0.59$	1.23
<b>5f</b>	$2.05 \pm 1.02$	2.88
Isoniazid	$0.36 \pm 0.09$	-1.02
Ethambutol	$5.01 \pm 0.17$	-0.38

<sup>a</sup>Drug-sensitive, <sup>b</sup>The values given are means of three experiments

The encouraging results of the anti-TB activity of novel triazolo[4,3-*a*]pyrazines (**5a-f**) against drug-sensitive Mtb H37Rv (ATCC 27294) strain prompted us to evaluate their broad

spectrum efficacy against two significant drug-resistant Mtb strains *viz.* Mtb H37Rv ATCC 35822 (INH-resistant) and Mtb H37Rv ATCC 35837 (ETH-resistant). When compared to INH (MIC > 100  $\mu\text{M}$ ), the synthesized compounds **5a-f** (MIC =  $20.83 \pm 0.67$  to  $61.92 \pm 0.18 \mu\text{M}$ ) were found to be more efficient in inhibiting the growth of INH-resistant Mtb H37Rv (ATCC 35822) strain. Similarly, when compared to ETH (MIC =  $19.57 \pm 0.42 \mu\text{M}$ ); compound **5c** (MIC =  $20.83 \pm 0.67 \mu\text{M}$ ) demonstrated similar, compounds **5d** (MIC =  $26.55 \pm 0.31 \mu\text{M}$ ), **5e** (MIC =  $32.71 \pm 0.69 \mu\text{M}$ ) and **5f** (MIC =  $39.59 \pm 0.35 \mu\text{M}$ ) displayed mild, while compounds **5a** (MIC =  $61.92 \pm 0.18 \mu\text{M}$ ) and **5b** (MIC =  $54.15 \pm 0.98 \mu\text{M}$ ) showed poor anti-TB activity against INH-resistant Mtb H37Rv (ATCC 35822) strain (Table-5). Moreover, the synthesized compounds **5a-f** (MIC =  $15.37 \pm 0.14$  to  $44.18 \pm 0.68 \mu\text{M}$ ) exhibited significantly potent anti-TB activity against ETH-resistant Mtb H37Rv (ATCC 35837) strain in comparison to ETH (MIC > 100  $\mu\text{M}$ ) but displayed poor activity compared to INH (MIC =  $0.31 \pm 0.06 \mu\text{M}$ ).

TABLE-5  
ANTI-TUBERCULAR ACTIVITY DATA OF **5a-f** AGAINST  
INH-RESISTANT Mtb H37Rv (ATCC 35822) AND  
ETH-RESISTANT Mtb H37Rv (ATCC 35837) STRAINS

Compound	MIC ( $\mu\text{M}$ ) <sup>a</sup>	
	INH-resistant Mtb H37Rv	ETH-resistant Mtb H37Rv
<b>5a</b>	$61.92 \pm 0.18$	$44.18 \pm 0.68$
<b>5b</b>	$54.15 \pm 0.98$	$35.44 \pm 0.35$
<b>5c</b>	$20.83 \pm 0.67$	$15.37 \pm 0.14$
<b>5d</b>	$26.55 \pm 0.31$	$21.03 \pm 0.16$
<b>5e</b>	$32.71 \pm 0.69$	$29.46 \pm 0.29$
<b>5f</b>	$39.59 \pm 0.35$	$31.18 \pm 0.72$
Isoniazid	> 100	$0.31 \pm 0.06$
Ethambutol	$19.57 \pm 0.42$	> 100

<sup>a</sup>The values given are means of three experiments.

**Structure-activity relationship (SAR):** The SAR studies revealed that a hydroxyl group attached to the *para*-position of the phenyl ring in compound **5c** (Table-3, entry 5c) is responsible for enhancing its activity against Mtb. The activity is significantly influenced by electron-donating substituents such as  $-\text{OH}$ ,  $-\text{NH}_2$  and  $-\text{OCH}_3$ . Thus, compounds **5d** and **5e** having  $-\text{NH}_2$  and  $-\text{OCH}_3$  groups, demonstrated substantial activity compared to compounds **5b** and **5f**, which have methyl and *t*-butyl groups, respectively. The activity was lower in compound **5a** owing to the absence of any substituent on the phenyl ring. It is evident from SAR analysis that electron donating substituents are responsible for increasing the activity of novel triazolo[4,3-*a*]pyrazines (**5b-f**).

**Cytotoxicity assay:** Cytotoxicity is an essential criterion for developing effective antibiotics and learning about the potential toxicity of newly found inhibitors. The cytotoxicity of novel triazolo[4,3-*a*]pyrazines (**5a-f**) was evaluated against the mammalian Vero cell line using the MTT cell viability test. Each experiment was performed in triplicate with isoniazid (INH) and ethambutol (ETH) used as controls. The results of cytotoxicity study indicated that the synthesized compounds **5a-f** are not cytotoxic at  $\text{IC}_{50} > 50 \mu\text{M}$  (Table-6). In addition,

TABLE-6  
CYTOTOXICITY OF TRIAZOLO[4,3-*a*]PYRAZINES (**5a-f**)  
AGAINST VERO CELLS AND THEIR SELECTIVITY INDEX (SI)

Compound	Cytotoxicity ( $\mu\text{M}$ ) <sup>a</sup>	Selectivity index		
		Mtb H37Rv	INH- resistant Mtb H37Rv	ETH- resistant Mtb H37Rv
<b>5a</b>	>50	8.17	0.80	1.13
<b>5b</b>	>50	15.92	0.92	1.41
<b>5c</b>	>50	84.74	2.40	3.25
<b>5d</b>	>50	51.54	1.88	2.37
<b>5e</b>	>50	39.06	1.53	1.69
<b>5f</b>	>50	24.39	1.26	1.60
Isoniazid	>50	138.88	0.5	161.29
Ethambutol	>50	9.98	2.55	0.5

INH: Isoniazid, ETH: Ethambutol

the selectivity index (SI) of each compound was calculated by the ratio logarithm of the  $\text{IC}_{50}$  and the MIC value for micro-organisms ( $\text{SI} = \log [\text{IC}_{50}/[\text{MIC}]]$ ) [44,45]. The SI values are employed in the evaluation of the *in vitro* efficacy of the tested compounds in the inhibition of the growth of bacteria or virus. Moreover, the higher selectivity index indicates that the drug is safer and efficient during *in vivo* treatment [46]. All synthesized compounds **5a-f** displayed lower SI values compared to INH ( $\text{SI} = 138.88$ ), while all compounds except **5a** ( $\text{SI} = 8.17$ ) exhibited higher SI values than ETH ( $\text{SI} = 9.98$ ) against drug-sensitive Mtb H37Rv (ATCC 27294) strain. Moreover, SI values of the synthesized compounds **5a-f** were found to be higher than INH ( $\text{SI} = 0.5$ ) and lower than ETH ( $\text{SI} = 2.55$ ) against INH-resistant Mtb H37Rv (ATCC 35822) strain. Similarly, the synthesized compounds **5a-f** demonstrated lower SI values than INH ( $\text{SI} = 161.29$ ) and higher SI values than ETH ( $\text{SI} = 0.5$ ) against ETH-resistant Mtb H37Rv (ATCC 35837) strain.

**Molecular docking:** Molecular docking simulations were performed to investigate and describe the interactions of novel

triazolo[4,3-*a*]pyrazines (**5a-f**) with the binding pocket of mycobacterial membrane protein large 3 (MmpL3) (PDB ID: 6AJJ) using AutoDock4.2. MmpL3 is a member of the superfamily of mycobacterial membrane proteins. It facilitates the transport of mycolic acid in the form of trehalose monomycolate from the cytoplasm to the periplasmic region, which is essential for the formation of mycobacterial cell walls. Thus, the compounds that can efficiently block MmpL3 can be developed into potential anti-TB agents. As a result, MmpL3 has been the target of several preclinical drugs for the treatment of MDR and XDR TB [47-49].

The results of the CASTp analysis indicated that the primary binding pocket of MmpL3, which encompasses the active site residues, possesses a volume of  $6227.6 \text{ \AA}^3$ , a pocket area of  $2657 \text{ \AA}^2$  and is comprised of six openings with a mouth area of  $894.9 \text{ \AA}^2$  each (Table-7). Novel triazolo[4,3-*a*]pyrazines (**5a-f**) demonstrated a favourable binding affinity towards the active site of the MmpL3 protein. The binding energies of the selected receptor (PDB ID: 6AJJ) with compounds **5a**, **5b**, **5c**, **5d**, **5e** and **5f** were found to be  $-7.41 \text{ kcal/mol}$ ,  $-6.48 \text{ kcal/mol}$ ,  $-6.11 \text{ kcal/mol}$ ,  $-5.84 \text{ kcal/mol}$ ,  $-6.49 \text{ kcal/mol}$  and  $-7.32 \text{ kcal/mol}$ , respectively. Compound **5a** displayed the highest binding affinity, while **5d** showed the lowest binding affinity (Table-8).

Furthermore, complexes (**6AJJ-5a-f**) were analyzed for hydrogen bonding and other interactions. In complex **6AJJ-5a**, the residue SER293 forms a hydrogen bond with 4th nitrogen atom of compound **5a**, whereas the residues ILE253, ASP256, TYR257, LEU259, PHE260, ASP645, TYR646, PHE649, LEU678, ALA682 are involved in hydrophobic and other interactions. Similarly, in complex **6AJJ-5b**, the residue SER652 forms a hydrogen bond with the oxygen atom of compound **5b**, whereas the residues PHE2, ARG288, THR289, PHE292, ALA582, ARG653 are involved in hydrophobic and other interactions. In complex **6AJJ-5c**, residue HIS913 forms a

TABLE-7  
CASTp ANALYSIS OF RECEPTOR MEMBRANE TRANSPORTER MmpL3 (PDB ID: 6AJJ)

POC:	Molecule ID	N_mth	Area_sa	Area_ms	Vol_sa	Vol_ms	Lenth	cnr
j_639044e9680dc	1	6	1955.644	2657.023	3073.077	6227.617	1430.767	643

TABLE-8  
HYDROGEN AND OTHER BONDING INTERACTIONS BETWEEN MEMBRANE TRANSPORTER MmpL3  
(PDB ID: 6AJJ) AND ALL COMPOUND COMPLEXES **6AJJ-5a**, **6AJJ-5b**, **6AJJ-5c**, **6AJJ-5d**, **6AJJ-5e**, **6AJJ-5f**

Complex	Binding affinity (kcal/mol)	No. of confirmation among 100	Hydrogen bond interaction	Hydrogen bond length ( $\text{\AA}$ )	Hydrophobic and other interactions
<b>6AJJ-5a</b>	-7.41	17	A: SER 293: OG $\leftrightarrow$ UNK1: N4	3.07	ILE253, ASP256, TYR257, LEU259, PHE260, ASP645, TYR646, PHE649, LEU678, ALA682
<b>6AJJ-5b</b>	-6.48	4	A: SER 652: N1 $\leftrightarrow$ UNK1: OG A: SER 652: N2 $\leftrightarrow$ UNK1: OG	2.84 2.92	PHE2, ARG288, THR289, PHE292, ALA582, ARG653
<b>6AJJ-5c</b>	-6.11	98	A: HIS 913: O $\leftrightarrow$ UNK1: O2	3.08	ARG7, GLU276, ALA277, ARG280, LYS896, ARG897, THR900, ALA909, PHE912, LEU914
<b>6AJJ-5d</b>	-5.84	90	A: HIS 913: ND1 $\leftrightarrow$ UNK1: O A: GLU 754: OE1 $\leftrightarrow$ UNK1: N5	2.53 2.73	ARG7, PHE750, ILE758, TYR910, GLU911, PHE912
<b>6AJJ-5e</b>	-6.49	48	A: SER 652: OG $\leftrightarrow$ UNK1: O2 A: ARG 653: NH1 $\leftrightarrow$ UNK1: O2 A: ARG 288: NH1 $\leftrightarrow$ UNK1: O1	3.33 2.90 3.13	PHE2, THR289, VAL291, PHE292, ALA582, VAL648
<b>6AJJ-5f</b>	-7.32	60	A: ARG 653: NH1 $\leftrightarrow$ UNK1: N3 A: SER 652: OG $\leftrightarrow$ UNK1: N4	3.24 2.69	MET1, ASN1, SER2, PHE2, GLN3, ARG288, THR289, PHE292, ALA582



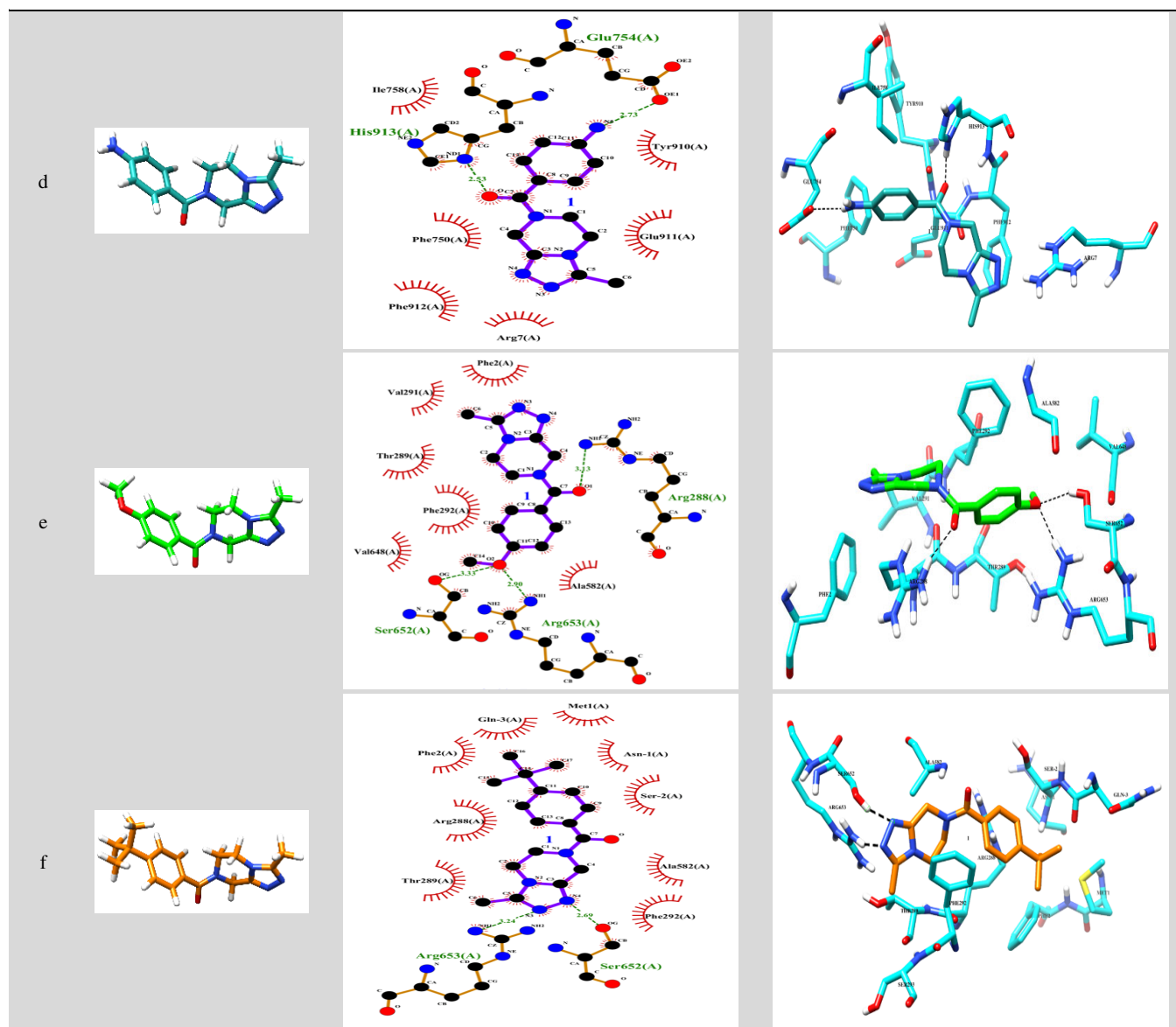


TABLE-10  
DRUG-LIKENESS PROPERTIES OF NOVEL TRIAZOLO[4,3-*a*]PYRAZINES (**5a-f**)

Compound	m.w.	Rotatable bonds	HBA	HBD	LogP	Molar refractivity	Log $K_p$ (cm/s)	TPSA ( $\text{\AA}^2$ )
<b>5a</b>	242.28	2	3	0	1.83	70.44	-7.41	51.02
<b>5b</b>	256.30	2	3	0	2.06	75.40	-7.23	51.02
<b>5c</b>	258.28	2	4	1	1.48	72.46	-7.75	71.25
<b>5d</b>	257.29	2	3	1	1.47	74.84	-7.98	77.04
<b>5e</b>	272.30	3	4	0	2.10	76.93	-7.61	60.25
<b>5f</b>	298.38	3	3	0	2.41	89.71	-6.56	51.02
Isoniazid	137.14	2	3	2	-0.97	35.13	-7.63	68.01
Ethambutol	204.31	9	4	4	2.46	58.11	-7.60	64.52
Lipinski rule	$\leq 500$	–	$< 10$	$< 10$	$< 5$	40-130	–	–

absorption of the drug. Novel triazolo[4,3-*a*]pyrazines (**5a-f**) exhibit low molecular weights in the range of 242 to 298 similar to the conventional anti-TB drugs such as isoniazid (INH, *m.w.* 137.14) and ethambutol (ETH, *m.w.* 204.31). In addition, the hydrogen bond acceptor (HBA) and donor (HBD) values of

the compounds **5a-f** ranging from 3 to 4 and 0 to 4, respectively are consistent with the values observed for INH and ETH. The logP values and the topological polar surface area (TPSA) values ( $< 140$ ) are essential to predict the good gastrointestinal absorption [51]. The logP values (1.48 to 2.41) of the synth-

TABLE-11  
*In silico* TOXICITY RISKS AND DRUG SCORES OF NOVEL TRIAZOLO[4,3-*a*]PYRAZINES (5a-f)

Compound	Toxicity risks				Drug likeness score	Drug score
	Mutagenic	Tumorigenic	Irritant	Reproductive effective		
5a	Not toxic	Not toxic	Not toxic	Not toxic	4.97	0.96
5b	Not toxic	Not toxic	Not toxic	Not toxic	3.85	0.94
5c	Not toxic	Not toxic	Not toxic	Not toxic	5.28	0.96
5d	Not toxic	Not toxic	Not toxic	Not toxic	5.47	0.96
5e	Not toxic	Not toxic	Not toxic	Not toxic	5.09	0.95
5f	Not toxic	Not toxic	Not toxic	Not toxic	-1.66	0.42
Isoniazid	Highly toxic	Highly toxic	Highly toxic	Highly toxic	-5.06	0.06
Ethambutol	Not toxic	Not toxic	Highly toxic	Not toxic	2.38	0.56

esized compounds **5a-f** were closer to that of ETH (logP = 2.46) rather than INH (logP = -0.97). Furthermore, the logKp values which determine the skin permeability were strikingly similar to the conventional anti-TB drugs and were found to be within an acceptable range [52]. Thus, *in silico* structure based analysis revealed that the synthesized novel triazolo[4,3-*a*]pyrazines (**5a-f**) exhibit the same drug-like properties as conventional anti-TB medicines and hence have the potential to be developed into powerful anti-TB agents. The OSIRIS property explorer programme [53] was also employed to predict the drug-likeness and drug score of novel triazolo[4,3-*a*]pyrazines (**5a-f**). All compounds demonstrated a significant and drug-likeness drug score (Table-11).

### Conclusion

A new series of triazolo[4,3-*a*]pyrazines (**5a-f**) via sequential oxidative cyclization, hydrogenation and potassium *tert*-butoxide assisted amidation of substituted methyl benzoates (**4a-f**). The synthesized compounds **5a-f** were successfully characterized by FT-IR, <sup>1</sup>H NMR and mass spectrometry. The novel triazolo[4,3-*a*]pyrazines (**5a-f**) exhibited notable efficacy in inhibiting the growth of drug-sensitive, isoniazid-resistant and ethambutol-resistant *Mycobacterium tuberculosis* (Mtb) H37Rv strains. Compound **5c** demonstrated significantly potent anti-tubercular activity compared to other compounds in the series. The molecular docking studies revealed strong binding with the active site of the target protein MmpL3. ADME analysis showed that triazolo[4,3-*a*]pyrazines (**5a-f**) exhibit good pharmacological parameters and do not contradict Lipinski's rule. The synthesized novel triazolo[4,3-*a*]pyrazines displayed drug-likeness properties and can be developed into potential anti-tubercular agents.

### ACKNOWLEDGEMENTS

We gratefully acknowledge the Indian Institute of Sciences (IISc), Bangalore, Sophisticated Analytical Instrumental Facility and Common Facility Center (CFC) Shivaji University, Kolhapur and Department of Microbiology, Shivaji University, Kolhapur for providing spectral and laboratory facilities.

### CONFLICT OF INTEREST

The authors declare that there is no conflict of interests regarding the publication of this article.

### REFERENCES

- M. Pai, M.A. Behr, D. Dowdy, K. Dheda, M. Divangahi, C.C. Boehme, A. Ginsberg, S. Swaminathan, M. Spigelman, H. Getahun, D. Menzies and M. Raviglione, *Nat. Rev. Dis. Primers*, **2**, 16076 (2016); <https://doi.org/10.1038/nrdp.2016.76>
- M.S. Raghu, C.B. Pradeep Kumar, K.N.N. Prasad, M.K. Prashanth, Y.K. Kumarswamy, S. Chandrasekhar and B. Veeresh, *ACS Comb. Sci.*, **22**, 509 (2020); <https://doi.org/10.1021/acscombsci.0c00038>
- A. Natarajan, P.M. Beena, A.V. Devnikar and S. Mali, *Indian J. Tuberc.*, **67**, 295 (2020); <https://doi.org/10.1016/j.ijtb.2020.02.005>
- C.J. Cambier, S. Falkow and L. Ramakrishnan, *Cell*, **159**, 1497 (2014); <https://doi.org/10.1016/j.cell.2014.11.024>
- M.S. Raghu, C.B. Pradeep Kumar, K. Yogesh Kumar, M.K. Prashanth, M.Y. Alshahrani, I. Ahmad and R. Jain, *Bioorg. Med. Chem. Lett.*, **60**, 128604 (2022); <https://doi.org/10.1016/j.bmcl.2022.128604>
- C. Vilchère and W.R. Jacobs Jr., *J. Mol. Biol.*, **431**, 3450 (2019); <https://doi.org/10.1016/j.jmb.2019.02.016>
- K.J. Seung, S. Keshavjee and M.L. Rich, *Cold Spring Harb. Perspect. Med.*, **5**, a017863 (2015); <https://doi.org/10.1101/cshperspect.a017863>
- Q.M. Trinh, H.L. Nguyen, T.N. Do, V.N. Nguyen, B.H. Nguyen, T.V.A. Nguyen, V. Sintchenko and B.J. Marais, *Int. J. Infect. Dis.*, **46**, 56 (2016); <https://doi.org/10.1016/j.ijid.2016.03.021>
- N. Kuroki, Y. Mochizuki and H. Mori, *J. Chem. Educ.*, **100**, 647 (2023); <https://doi.org/10.1021/acs.jchemed.2c00837>
- J.A. Keith, V. Vassilev-Galindo, B. Cheng, S. Chmiela, M. Gastegger, K.-R. Müller and A. Tkatchenko, *Chem. Rev.*, **121**, 9816 (2021); <https://doi.org/10.1021/acs.chemrev.1c00107>
- Y.F. Shi, Z.X. Yang, S. Ma, P.L. Kang, C. Shang, P. Hu and Z.P. Liu, *Engineering*, **27**, 70 (2023); <https://doi.org/10.1016/j.eng.2023.04.013>
- X. Yuan, L. Li, Z. Shi, H. Liang, S. Li and Z. Qiao, *Adv. Powd. Mat.*, **1**, 100026 (2022); <https://doi.org/10.1016/j.apmate.2021.12.002>
- F. Pan, A.T. Jalil, F. Alsaikhan, M. Adil, A.J. Kadhim, D.A.A. Amran, M. Abosaooda, A.S. Altamimi, S.M.D. Younis, A.N.K. Lup, S. Tavassoli, H. Balakheyli and A. Soltani, *Diamond Rel. Mater.*, **136**, 110044 (2023); <https://doi.org/10.1016/j.diamond.2023.110044>
- L. Pinzi and G. Rastelli, *Int. J. Mol. Sci.*, **20**, 4331 (2019); <https://doi.org/10.3390/ijms20184331>
- A. Abdolmaleki, F. Shiri and J.B. Ghasemi, Use of Molecular Docking as a Decision-Making Tool in Drug Discovery, In: *Molecular Docking for Computer-Aided Drug Design*, Academic Press, Chap. 11, pp. 229-243 (2020).
- G.M. Morris and M. Lim-Wilby, *Methods Mol. Biol.*, **443**, 365 (2008); [https://doi.org/10.1007/978-1-59745-177-2\\_19](https://doi.org/10.1007/978-1-59745-177-2_19)
- X.-Y. Meng, H.-X. Zhang, M. Mezei and M. Cui, *Curr. Computeraided Drug Des.*, **7**, 146 (2011); <https://doi.org/10.2174/157340911795677602>

18. A. Gomtsyan, *Chem. Heterocycl. Compd.*, **48**, 7 (2012); <https://doi.org/10.1007/s10593-012-0960-z>
19. N. Kerru, L. Gummidi, S. Maddila, K.K. Gangu and S.B. Jonnalagadda, *Molecules*, **25**, 1909 (2020); <https://doi.org/10.3390/molecules25081909>
20. N. Tambat, S.K. Mulani, A. Ahmad, S.B. Shaikh and K. Ahmed, *Russ. J. Bioorg. Chem.*, **48**, 865 (2022); <https://doi.org/10.1134/S1068162022050259>
21. R. Raveesha, K.Y. Kumar, M.S. Raghu, S.B.B. Prasad, A. Alsalmeh, P. Krishnaiah and M.K. Prashanth, *J. Mol. Struct.*, **1255**, 132407 (2022); <https://doi.org/10.1016/j.molstruc.2022.132407>
22. D.J. Jethava, M.A. Borad, M.N. Bhoi, P.T. Acharya, Z.A. Bhavsar and H.D. Patel, *Arab. J. Chem.*, **13**, 8532 (2020); <https://doi.org/10.1016/j.arabj.2020.09.038>
23. D.P. Hiwarale, W.B. Chandane, S.M. Deshmukh, S.M. Arde, V.D. Sonawane, M.G. Kukade, N.M. Naik, K.D. Sonawane, G.S. Rashinkar and S.G. Sonkamble, *J. Mol. Struct.*, **1286**, 135556 (2023); <https://doi.org/10.1016/j.molstruc.2023.135556>
24. M.G. Kukade, U.N. Pol, R.P. Kagne, W.B. Chandane, A.J. Bodake, M.K. Prashanth, K.Y. Kumar and M.S. Raghu, *J. Indian Chem. Soc.*, **99**, 100509 (2022); <https://doi.org/10.1016/j.jics.2022.100509>
25. P.J. Nelson and K.T. Potts, *J. Org. Chem.*, **27**, 3243 (1962); <https://doi.org/10.1021/jo01056a061>
26. O.R. Thiel and M.M. Achmatowicz, *Org. Synth.*, **90**, 287 (2013); <https://doi.org/10.15227/orgsyn.090.0287>
27. G. Hu, C. Wang, X. Xin, S. Li, Z. Li, Y. Zhao and P. Gong, *New J. Chem.*, **43**, 10190 (2019); <https://doi.org/10.1039/C9NJ02154J>
28. J. Park, Y.-J. Yoon, B. Kim, H.-G. Lee, S.-B. Kang, G. Sung, J.-J. Kim and S.-G. Lee, *Synthesis*, **44**, 42 (2012); <https://doi.org/10.1055/s-0031-1289622>
29. M. Madaiah, M.K. Prashanth, H.D. Revanasiddappa and B. Veeresh, *New J. Chem.*, **40**, 9194 (2016); <https://doi.org/10.1039/C6NJ02069K>
30. C.B.P. Kumar, M.S. Raghu, B.S. Prathibha, M.K. Prashanth, K.Y. Kumar, G. Kanthimathi, L. Parashuram and F.A. Alharthi, *Bioorg. Med. Chem. Lett.*, **44**, 128118 (2021); <https://doi.org/10.1016/j.bmcl.2021.128118>
31. H.M. Berman, J. Westbrook, Z. Feng, G. Gilliland, T.N. Bhat, H. Weissig, I.N. Shindyalov and P.E. Bourne, *Nucleic Acids Res.*, **28**, 235 (2000); <https://doi.org/10.1093/nar/28.1.235>
32. B. Zhang, J. Li, X. Yang, L. Wu, J. Zhang, Y. Yang, Y. Zhao, L. Zhang, X. Yang, X. Yang, X. Cheng, Z. Liu, B. Jiang, H. Jiang, L.W. Guddat, H. Yang and Z. Rao, *Cell*, **176**, 636 (2019); <https://doi.org/10.1016/j.cell.2019.01.003>
33. G.M. Morris, R. Huey, W. Lindstrom, M.F. Sanner, R.K. Belew, D.S. Goodsell and A.J. Olson, *J. Comput. Chem.*, **30**, 2785 (2009); <https://doi.org/10.1002/jcc.21256>
34. A. Axenopoulos, P. Daras, G.E. Papadopoulos and E.N. Houstis, *IEEE/ACM Trans. Comput. Biol. Bioinformatics*, **10**, 135 (2013); <https://doi.org/10.1109/TCBB.2012.149>
35. R.S. Parulekar, S.H. Barage, C.B. Jalkute, M.J. Dhanavade, P.M. Fandilolu and K.D. Sonawane, *Protein J.*, **32**, 467 (2013); <https://doi.org/10.1007/s10930-013-9506-1>
36. C.B. Jalkute, S.H. Barage, M.J. Dhanavade and K.D. Sonawane, *Protein J.*, **32**, 356 (2013); <https://doi.org/10.1007/s10930-013-9492-3>
37. M.J. Dhanavade, C.B. Jalkute, S.H. Barage and K.D. Sonawane, *Comput. Biol. Med.*, **43**, 2063 (2013); <https://doi.org/10.1016/j.compbiomed.2013.09.021>
38. S.B. Paymal, S.S. Barale, S.V. Supanekar and K.D. Sonawane, *Comput. Biol. Med.*, **159**, 106965 (2023); <https://doi.org/10.1016/j.compbiomed.2023.106965>
39. W. Tian, C. Chen, X. Lei, J. Zhao and J. Liang, *Nucleic Acids Res.*, **46**(W1), W363 (2018); <https://doi.org/10.1093/nar/gky473>
40. E.F. Pettersen, T.D. Goddard, C.C. Huang, G.S. Couch, D.M. Greenblatt, E.C. Meng and T.E. Ferrin, *J. Comput. Chem.*, **25**, 1605 (2004); <https://doi.org/10.1002/jcc.20084>
41. A.C. Wallace, R.A. Laskowski and J.M. Thornton, *Protein Eng. Des. Sel.*, **8**, 127 (1995); <https://doi.org/10.1093/protein/8.2.127>
42. R.A. Laskowski and M.B. Swindells, *J. Chem. Inf. Model.*, **51**, 2778 (2011); <https://doi.org/10.1021/ci200227u>
43. C.A. Lipinski, *Drug Discov. Today. Technol.*, **1**, 337 (2004); <https://doi.org/10.1016/j.ddtec.2004.11.007>
44. B.C. Nunes, M.M. Martins, R. Chang, S.A.L. Morais, E.A. Nascimento, A. de Oliveira, L.C.S. Cunha, C.V. da Silva, T.L. Teixeira, M.A.L.V. Ambrósio, C.H.G. Martins and F.J.T. de Aquino, *Ind. Crops Prod.*, **92**, 277 (2016); <https://doi.org/10.1016/j.indcrop.2016.08.016>
45. G. Indrayanto, G.S. Putra and F. Suhud, *Profiles Drug Subst. Excip. Relat. Methodol.*, **46**, 273 (2021); <https://doi.org/10.1016/bs.podrm.2020.07.005>
46. J.C. Pritchett, L. Naesens, J. Montoya, eds.: L. Flamand, I. Lautenschlager, G. Krueger and D. Ablashi, Treating HHV-6 Infections: The Laboratory Efficacy and Clinical Use of Anti-HHV-6 Agents, In: Human Herpesviruses HHV-6A, HHV-6B, and HHV-7: Diagnosis and Clinical Management, Elsevier, edn. 3, pp. 311-331 (2014); <https://doi.org/10.1016/B978-0-444-62703-2.00019-7>
47. J.R. Bolla, *Biochem. Soc. Trans.*, **48**, 1463 (2020); <https://doi.org/10.1042/BST20190950>
48. M.D. Umare, P.B. Khedekar and R.V. Chikhale, *ChemMedChem*, **16**, 3136 (2021); <https://doi.org/10.1002/cmdc.202100359>
49. M. Shao, M. McNeil, G.M. Cook and X. Lu, *Eur. J. Med. Chem.*, **200**, 112390 (2020); <https://doi.org/10.1016/j.ejmech.2020.112390>
50. C.A. Lipinski, F. Lombardo, B.W. Dominy and P.J. Feeney, *Adv. Drug Deliv. Rev.*, **46**, 3 (2001); [https://doi.org/10.1016/S0169-409X\(00\)00129-0](https://doi.org/10.1016/S0169-409X(00)00129-0)
51. J. Ali, P. Camilleri, M.B. Brown, A.J. Hutt and S.B. Kirton, *J. Chem. Inf. Model.*, **52**, 420 (2012); <https://doi.org/10.1021/ci200387c>
52. M. Rudrapal, D. Chetia and V. Singh, *J. Enzyme Inhib. Med. Chem.*, **32**, 1159 (2017); <https://doi.org/10.1080/14756366.2017.1363742>
53. T. Sander, J. Freyss, M. Von Korff, J.R. Reich and C. Rufener, *J. Chem. Inf. Model.*, **49**, 232 (2009); <https://doi.org/10.1021/ci800305f>